 ©2016 Kvantovaya Elektronika and Turpion Ltd

LASER BEAMS

DOI: 10.1070/QEL15880

Control of the formation of vortex Bessel beams in uniaxial crystals by varying the beam divergence

V.D. Paranin, S.V. Karpeev, S.N. Khonina

Abstract. **The transformation of zero-order Bessel beams into a second-order vortex Bessel beam in $CaCO_3$ and $LiNbO_3$ crystals is experimentally studied, and a possibility of controlling the beam transformation by changing the wavefront curvature of the illuminating beam is shown. A quasi-periodic nature of the Bessel beam transformation in a crystal while illuminating the diffraction axicon by a convergent beam is observed.**

Keywords: *Bessel laser beams, diffraction axicon, uniaxial crystal, wavefront curvature, telescopic optical system.*

1. Introduction

The formation of higher-order Bessel beams, namely vortex Bessel beams, represents an urgent task for a number of applications, including optical manipulation tasks [1–3]. Preparation of such beams by means of diffraction optical elements (DOEs) encounters certain difficulties because of the formation of the vortex phase component. In this case, manufacturing a DOE with a multilevel micro-relief is required [4], which is technologically challenging to implement with high accuracy [5]. The DOEs with a comparatively small number of levels allow accurate generation of vortex beams if they represent the analogues of holograms with a reference beam. Herewith, the formation occurs in several off-axis orders, which limits the energy efficiency [6, 7]. At the same time, the binary annular gratings (phase and amplitude diffraction axicons) allow obtaining zero-order Bessel beams along the optical axis.

One of the ways in the development of the devices and methods for producing vortex Bessel beams is the use of anisotropic crystals. Theoretical and experimental studies [8–12] have shown that, in uniaxial crystals, the zero-order Bessel beam, which propagates along the crystal axis, periodically transforms into the second-order vortex Bessel beam. A complete transformation requires that the crystal thickness is a multiple of the transformation period. As shown in [8], the repetition period of the beam shape in a crystal depends on the refractive indices of the crystal and the numerical aperture of the axicon, the period constituting tens of microns for the axicons with a numerical aperture of 0.15–0.5. The micron-sized tolerances of the crystal thickness must be maintained to form a predetermined beam, which is rather difficult because of high complexity of manufacturing and variation of the crystal properties. In this paper we propose to perform matching of the beam transformation period with the crystal length by means of varying the wavefront curvature of the beam illuminating the axicon. It is known that supplementing the axicon by a lens [13] allows the formation of the Bessel beams with a varying spatial frequency [14]. We consider two configurations of optical implementation of the dynamic matching of the transformation period in the crystal at the expense of the changes in the spatial frequency of the Bessel beam.

V.D. Paranin Samara State Aerospace University, Moskovskoe sh. 34, 443086 Samara, Russia; e-mail: vparanin@mail.ru;
S.V. Karpeev, S.N. Khonina Samara State Aerospace University, Moskovskoe sh. 34, 443086 Samara, Russia; Image Processing Systems Institute, Russian Academy of Sciences, Molodogvardeiskaya ul. 15, 443001 Samara, Russia; e-mail: karp@smr.ru, khonina@smr.ru

Received 13 June 2015; revision received 17 November 2015
Kvantovaya Elektronika **46** (2) 163–168 (2016)
Translated by M.A. Monastyrskiy

2. Theoretical justification

The electric field intensity in the Bessel beam of an arbitrary order m is described by the formula [1]

$$E(r,\varphi) = J_m(k\alpha r)\exp(im\varphi), \quad (1)$$

where $J_m(x)$ is the Bessel function of mth order; $k = 2\pi/\lambda$ is the wavenumber; α is the numerical aperture; and r,φ are the polar coordinates.

At $m = 0$ the Bessel beam is known as a classical diffraction-free beam, which is formed by the axicon and has a maximal intensity at the centre. At $m \neq 0$, as is seen from (1), the exponential factor $\exp(im\varphi)$ describing the vortex phase appears. Thus, the intensity value vanishes on the optical axis. This phenomenon is associated with the 'phase dislocations' or 'phase singularities', since the light wave phase is not defined at the vortex beam centre and may take any value from zero to 2π. The main property of the spiral phase dislocation consists in the fact that a circumvention of the dislocation over the wavefront surface changes the phase strictly by 2π. Depending on the phase vortex direction, spiral dislocations are divided into the left-hand (negative) and right-hand (positive) dislocations.

It is assumed that the optical vortex is a result of the superposition of two or more light beams (in particular, monochromatic beams), which in a definite way balance each other, so that the wave maxima of one beam overlap the wave minima of the other, thus forming the zero-intensity region mentioned above. The passage of the zero-order Bessel beams through an anisotropic crystal results in the emergence of ordinary and extraordinary rays overlapping in the nonparaxial case, which, as indicated above, leads to the formation of an optical vortex.

The intensity distribution $I(x,y,z)$ in the Bessel beam propagation along the crystal axis appears as [11, 12]:

$$I(x,y,z) \approx \frac{1}{2}[|C(z)|^2 J_0^2(\alpha k\sqrt{x^2+y^2}) + |S(z)|^2 J_2^2(\alpha k\sqrt{x^2+y^2})], \quad (2)$$

where

$$C(z) = \exp(ikz\gamma_o) + \exp(ikz\gamma_e),$$

$$S(z) = \exp(ikz\gamma_o) - \exp(ikz\gamma_e);$$

the values $\gamma_o = \sqrt{n_o^2 - \alpha^2}$ and $\gamma_e = \sqrt{n_o^2 - \alpha^2 n_o^2/n_e^2}$ determine the propagation direction of the ordinary and extraordinary rays; n_o, n_e are the crystal refractive indices for the ordinary and extraordinary rays, respectively; and z is the travelled distance.

A complete transformation of the zero-order Bessel beam into the second-order vortex Bessel beam occurs periodically at the distances that are multiple of

$$z_p = \frac{\lambda}{\gamma_o - \gamma_e} \approx \frac{2\lambda n_o n_e^2}{\alpha^2(n_o^2 - n_e^2)}. \quad (3)$$

As follows from (3), the complete transformation period depends on the crystal refractive indices, the axicon numerical aperture and the radiation wavelength. To dynamically change (adjust) the period, it is proposed to vary the parameter α by changing the wavefront curvature of the beam illuminating the axicon.

As a rule, it is assumed that the axicon is illuminated by a plane-parallel beam, and the larger the diameter of the beam illuminating the axicon, the more extended the light segment being formed. In most cases, a plane-parallel beam is obtained by means of the beam expander that represents a telescopic system enlarging the laser beam size. In contrast, we propose to coordinate the beam transformation period with the crystal length by varying the wavefront curvature of the illuminating beam. Two configurations are possible in this case.

The first configuration involves the use of a beam expander which generates a spherical wavefront by changing the distance between the telescopic system's lenses. The binary axicon produces two diffraction orders that form both converging and diverging wavefronts. This configuration uses the convergent diffraction order the axicon generates. Illumination of the axicon with a spherical wavefront is equivalent to summation of the phase functions of the axicon and the lens (this element is known as 'linsacon' [13]). Depending on the wavefront curvature radius of the beam illuminating the axicon, the numerical aperture of the formed Bessel beam, which determines the distance between the rings, will vary. Consequently, the beam transformation period in the crystal will also vary. Such an adjustment is possible in regard to the formation of both divergent (the period is increased) and convergent (the period is decreased) spherical wavefronts.

In case of propagation in free space, the Bessel beam spatial frequency (scale) changes in accordance with the travelled distance and the wavefront curvature [14]:

$$I(x,y,z) = \frac{z\alpha_0^2 f^3}{\lambda(f-z)^3} J_0^2[k\alpha(z)\sqrt{x^2+y^2}], \quad (4)$$

where α_0 is the axicon spatial frequency (corresponding to the Bessel beam frequency when illuminated by a plane wave); f is focal distance of the lens used to form a spherical wavefront; and $\alpha(z) = \alpha_0 f/(f-z)$ is a variable frequency of the quasi-Bessel beam being formed.

The second configuration corresponds to the case when the axicon is illuminated by a planar beam emerging from the expander; then, the beam is transformed by an additional lens positioned behind the axicon. In this case, a diverging diffraction order formed by the axicon is used, and we come to the use of the lens as the imaging system that forms a real image. A certain cross section of the axicon focal region is located in the object plane of the lens, and the image plane is positioned within the crystal in such a way that a complete transformation occurs at the crystal output. In this case, the spatial frequency (scale) of the imaged Bessel beam is also varied [3].

The main drawback of this approach is that the transformation period varies in the course of light propagation inside the crystal. Since the axicon forms an extended light segment along the optical axis, different parts of the segment are imaged within the crystal with different magnifications due to the changes in the ratios between the optical system distances. This effect is clearly visible in the images obtained in the modelling process and presented in the next section (see, for example, Fig. 3). It is seen that the repetition period of the beam shape is changed along the optical axis, and the process is quasi-periodic in this case. This leads to the fact that the periods of rings at the input and output of the crystal are different. However, these effects are insignificant at small enough magnifications and moderate numerical apertures.

3. Numerical simulation

Simulation of the Bessel beam propagation in a uniaxial crystal has been conducted by means of the method of expansion in plane waves, set forth in [11, 12]. The period of the amplitude diffraction axicon is set equal to 4 μm, the $LiNbO_3$ crystal thickness is 0.554 mm, the refractive indices are $n_o = 2.286$, $n_e = 2.200$ and the wavelength is $\lambda = 632.8$ nm. The calculated intensity distributions at the crystal output along the propagation axis for different wavefronts are shown in Figs 1, 2 (the near-axis parts of the beams are displayed).

The results of simulation show that the Bessel beam's transformation period constitutes hundreds of micrometres. This allows manufacturing of miniature beam transducers on the basis of thin crystals, on the surface of which a diffraction axicon is formed. The use of a complementary lens leads to a quasi-periodic dependence of the Bessel beam transformation in the crystal along the propagation axis. This is particularly well-observed for a convergent beam, a decrease in the transformation period along the propagation axis being accompanied by a change in the transversal scale of the beam (Fig. 3).

For a convergent beam, the transformation period decreases with increasing distance from the crystal input surface, whilst for divergent beam it increases. Therefore, the use of a movable lens extends the possibility of beam transformation, since in this case both the scale and transverse intensity distribution can be varied.

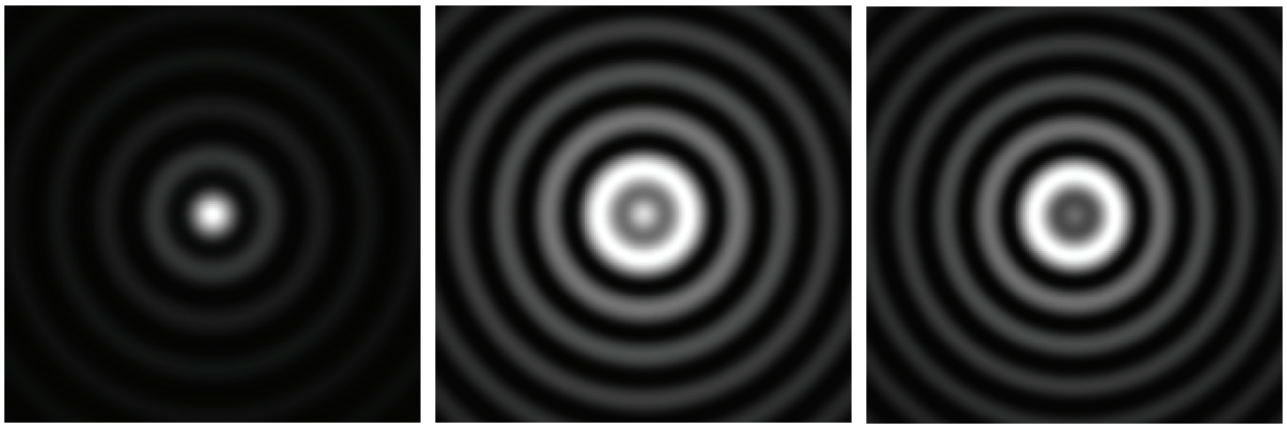

Figure 1. Calculated intensity distributions at the $LiNbO_3$ crystal output at the distances between the objective lens and lens L1 (see Fig. 4): (a) 0, (b) 10 and (c) 20 cm.

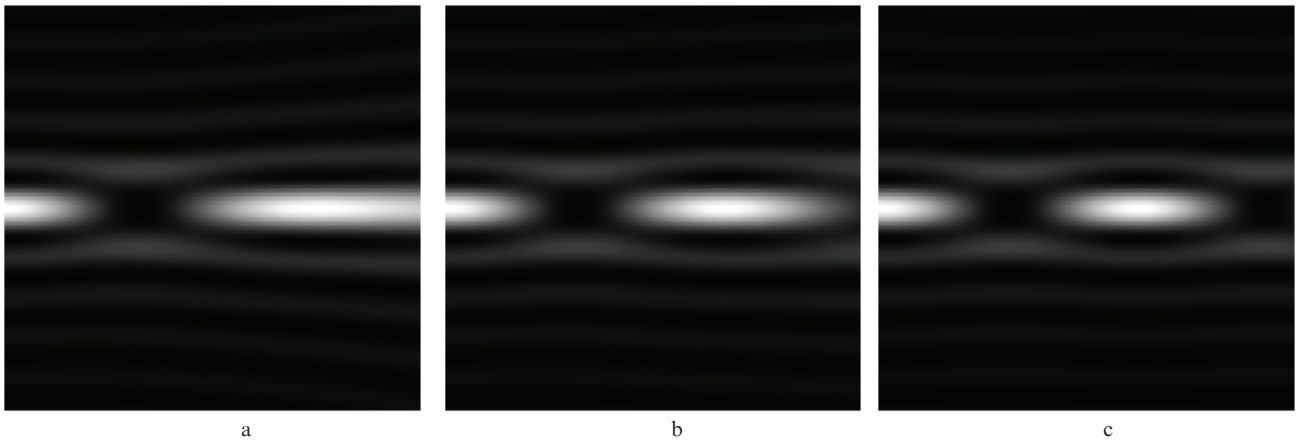

Figure 2. Calculated intensity distributions along the propagation axis at the distances between the objective lens and lens L1: (a) 0, (b) 10 and (c) 20 cm.

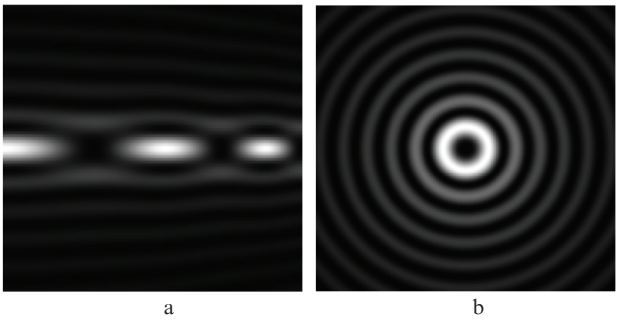

Figure 3. Calculated intensity distributions (a) along the propagation axis and (b) at the crystal output in illuminating the axicon by a converging beam.

4. Experimental study

To investigate the optical-mechanical transformation of the zero-order Bessel beam into the second-order vortex beam, an optical setup has been assembled, the schematic of which is shown in Fig. 4. The setup comprises a radiation source, a beam expander, a diffraction axicon, a crystal, a microlens and a CCD. To measure the wavefront, a Hartmann sensor and an optical-quality beam splitter were used. The crystal axis was oriented parallel to the optical axis of the scheme. A two-dimensional angular frame was used to ensure exact alignment of the crystal axis with the system optical axis.

To form the zero-order Bessel beam on a glass substrate, an amplitude diffraction axicon was manufactured, with a 40-mm diameter and a period of rings of 4 μm, which corresponds to the angular aperture $\alpha = 0.159$ for $\lambda = 0.6328$ μm. The photoresist mask exposure was carried out using the CLWS-200 installation in vector mode, which ensured the

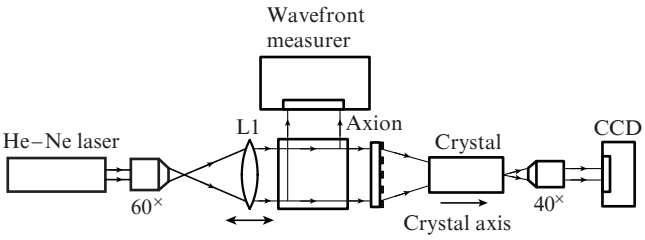

Figure 4. Experimental setup.

absence of step topology defects and high quality of the thus formed Bessel beam. A photograph of the diffraction mask (strips of chromium of 100 nm in thickness) obtained with an electron microscope is shown in Fig. 5. The width of the light and dark rings is the same and constitutes 2 μm. Two rings with enlarged width, located in the central part of the axicon, are required for the laser beam alignment. Since the radius of the outer wide ring of chromium does not exceed 50 μm, the distortion this ring introduces into the Bessel beam is observed at the distances up to 350 μm at the aperture $\alpha = 0.159$. Given the crystal is distanced by 5 mm from the axicon and the diameter of illuminated axicon area is 15 mm, the presence of such defects does not affect the results of experiments.

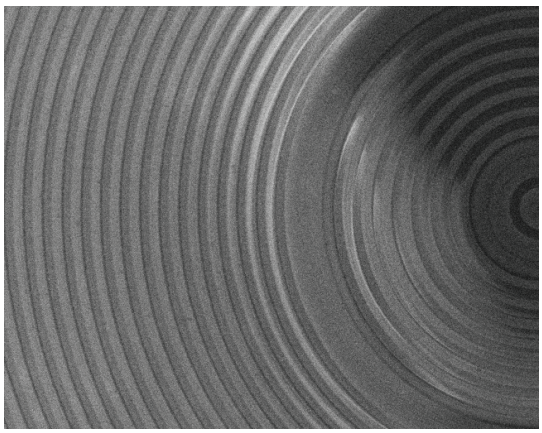

Figure 5. Photograph of the diffraction axicon with a period of rings of 4 μm.

The increase in the beam sizes at the crystal output is provided by a $40^{\times}$ objective lens with an aperture NA = 0.65 exceeding the axicon aperture. The laser beam expansion is performed by a $60^{\times}$ lens and a plano-convex lens L1 with a focal length of 15 cm. The lens L1 was capable of moving along the optical axis, thus providing a change in the curvature of the wavefront illuminating the axicon. Figure 6A shows experimental results of the Bessel beam transformation in the $CaCO_3$ crystal with a length of 15 mm at different positions of the lens L1, while Fig. 6B demonstrates the corresponding wavefronts of the illuminating beam. The presence of the zero- and second-order Bessel beams at the crystal output, described theoretically in [12], corresponds to the experimentally observed intensity distributions. The vortex nature of the second-order Bessel beam formed at the output from a uniaxial crystal was proved earlier in [11] using the output beam interferogram (Fig. 7). It is known that spiral dislocation leads to emergence of a so-called 'fork' in the finite-width fringes of the interferogram, with a centre in the dislocation region, those fringes being a result of interaction of the wavefront under study with a tilted planar wavefront. This 'fork' looks like a branching of a single fringe into m fringes, where m indicates the vortex order. Indeed, one can observe a double fork at the centre of the interferogram shown in Fig. 7, which indicates the presence of the second-order vortex beam component.

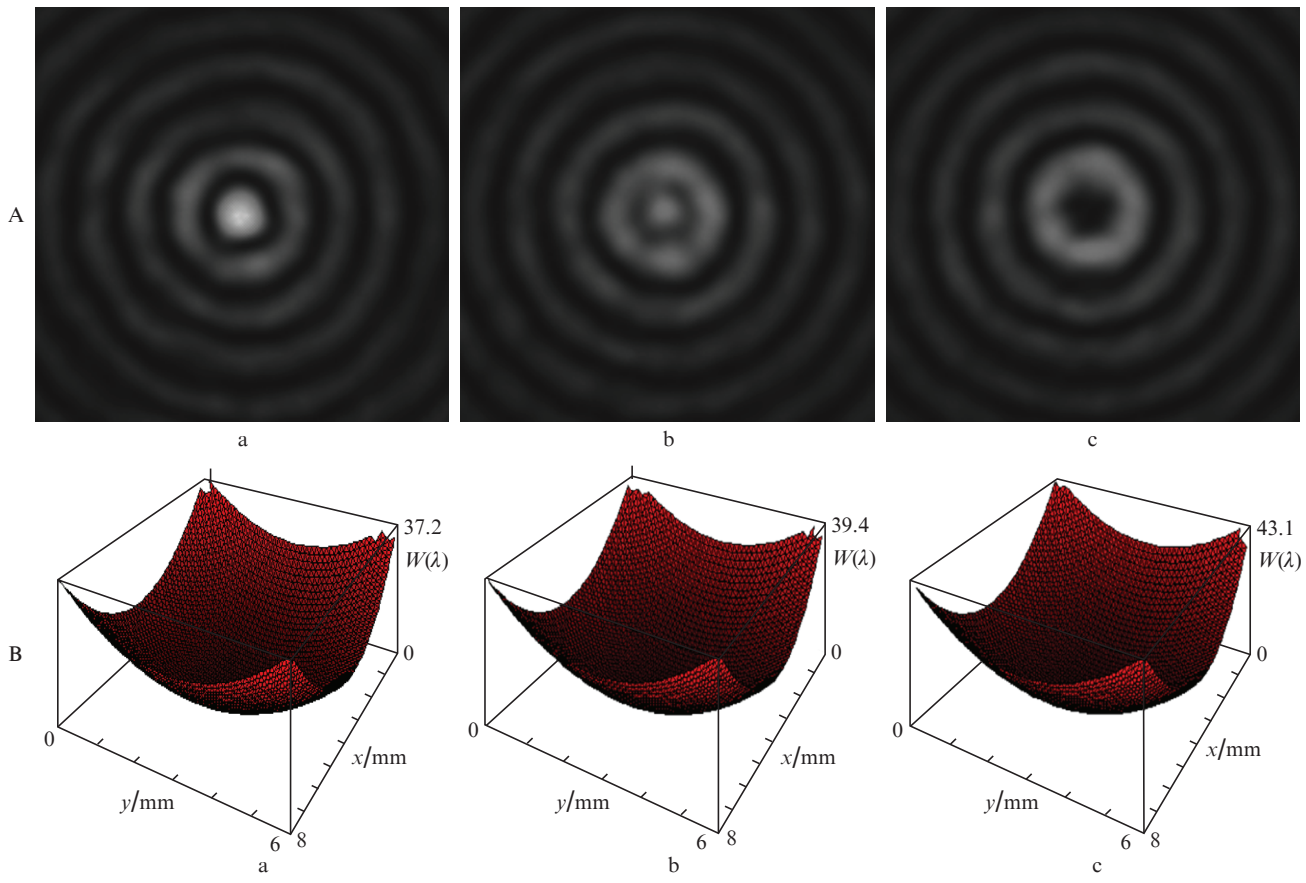

Figure 6. (A) Measured intensity distributions at the $CaCO_3$ crystal output and (B) the wavefronts of illuminating beams at the distances between the objective lens and the lens L1: (a) 18, (b) 18.5 and (c) 19 cm.

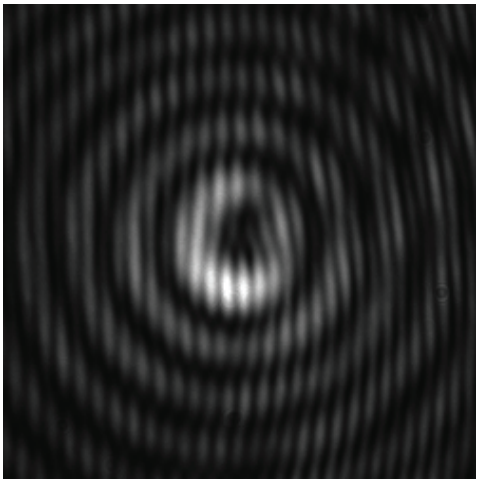

Figure 7. Output beam interferogram.

A very urgent problem is to reduce the overall sizes of the device, which requires reducing the transformation period. It is clear from preceding consideration that the transformation period can be reduced by increasing the axicon numerical aperture. To solve this problem, experiments with a diffraction axicon having a period of rings of 2 μm have been carried out. Since the axial segment length of such an axicon is not large, the $LiNbO_3$ crystal with a thickness of only 0.554 ± 0.002 mm was used. To increase the beam diameter and the axial segment length, the lens L1 with a focal length of 15 cm was replaced by a lens with a focal length of 20 cm. The transformation results and relevant wavefronts are shown in Fig. 8.

As it follows from the data in Figs 6–8, a change in the wavefront curvature allows the zero-order Bessel beam to be transformed into the second-order vortex beam. This transformation may employ both concave and convex wavefronts that correspond to converging and diverging beams. Thus, the displacement magnitude being required for complete transformation is determined by the crystal length, birefringence indices and numerical aperture of the axicon. The experimental results are in good agreement with the data predicted by numerical simulation.

5. Conclusions

We have experimentally studied the propagation of the zero-order Bessel beam formed by a diffraction axicon along the uniaxial crystal axis. A mutual transformation of the zero- and second-order Bessel beams in the crystal by means of the collimator lens displacement is shown. A possibility is specified for periodic and quasi-periodic Bessel beam transformation determined by the wavefront curvature of the illuminating beam.

It is found that the diffraction axicon with a period of a few micrometres allows one to obtain a transformation period of hundreds micrometres of the Bessel beam in a crystal (in

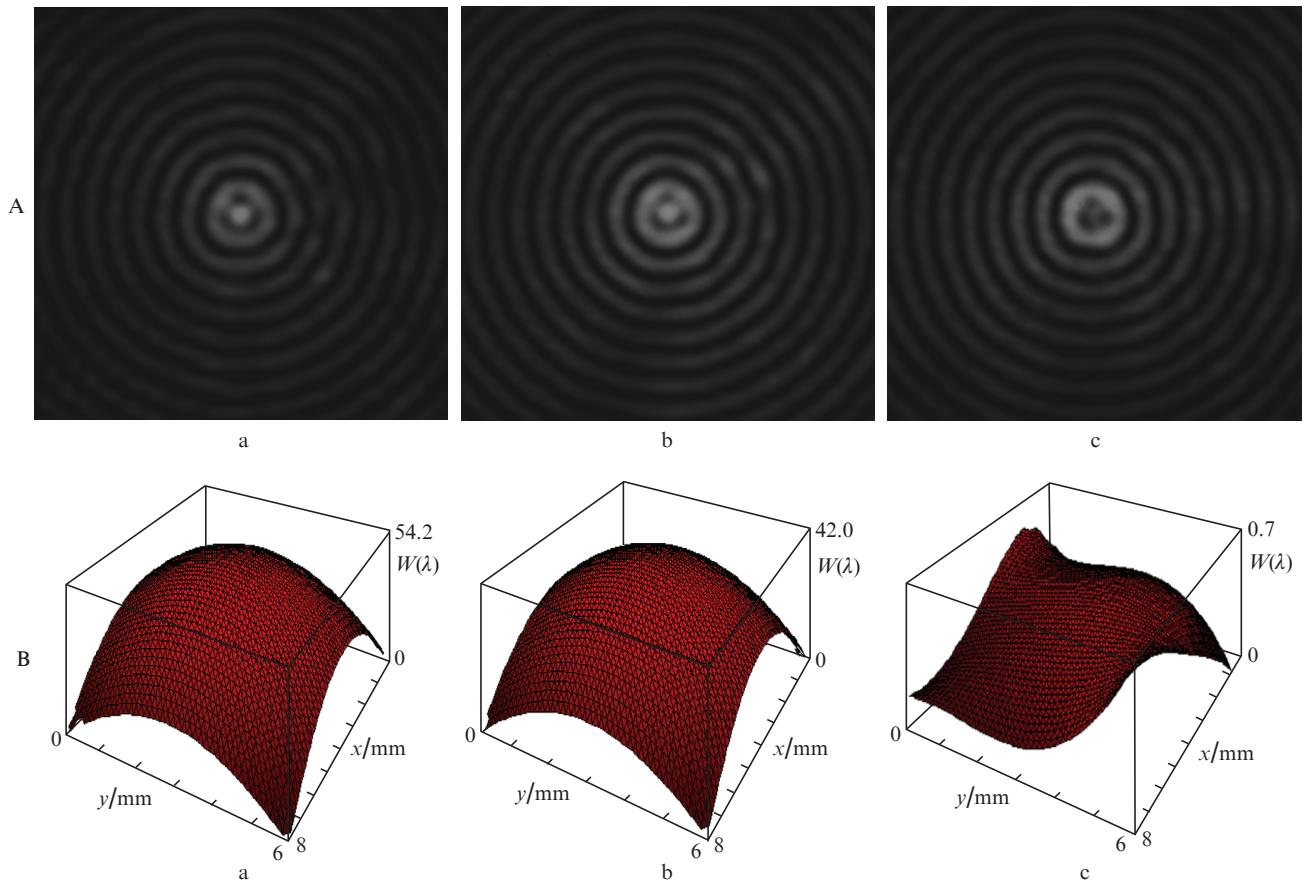

Figure 8. (A) Measured intensity distributions at the $LiNbO_3$ crystal output and (B) the wavefronts of illuminating beams at the distances between the objective lens and lens L1: (a) 0, (b) 10 and (c) 20 cm.

the visible wavelength range). This makes it possible to design miniature beam transducers based on thin uniaxial crystals, on the surface of which a diffraction micro-relief is formed.

A comparison of the optical-mechanical approach with other possible methods of adjusting to the crystal parameters, including heating the crystal and varying the wavelength, reveals undoubted advantages of the optical-mechanical approach due to the ease of implementation and broadness of the tuning range.

A variation of the spatial transformation period by means of a movable lens changes the output beam sensitivity to the optical system parameters, such as the wavelength, crystal birefringence, position of optical elements, etc., which allows setting the starting working point of the beam transducer and tuning its sensitivity to external influences. Given the processability and low cost of such transducers, this makes it possible to use them in the measurement technique.

Acknowledgements. The work was supported by the Russian Science Foundation (Grant No. 14-19-00114).

References

1. Bouchal Z. *Czech. J. Phys*., **53** (7), 537 (2003).
2. Soifer V.A., Kotlyar V.V., Khonina S.N. *Physics of Particles and Nuclei*, **35** (6), 733 (2004).
3. Khonina S.N., Kotlyar V.V., Skidanov R.V., Soifer V.A., Jefimovs K., Simonen J., Turunen J. *J. Modern Opt*., **51** (14), 2167 (2004).
4. Kotlyar V.V., Almazov A.A., Khonina S.N., Soifer V.A., Elfstrom H., Turunen J. *J. Opt. Soc. Am. A*, **22** (5), 849 (2005).
5. Tsai H.Y., Smith H.I., Menon R. *J. Vac. Sci. Technol. B*., **25** (6), 2068 (2007).
6. Vasara A., Turunen J., Friberg A.T. *J. Opt. Soc. Am. A*, **6**, 1748 (1989).
7. Golovashkin D.L., Kotlyar V.V., Soifer V.A., Doskolovich L.L., Kazanskiy N.L., Pavelyev V.S., Khonina S.N., Skidanov R.V. *Computer Design of Diffractive Optics* (Cambridge: Woodhead Pub. Ltd., 2012).
8. Khilo N.A., Ryzhov A.A., Petrova E.S. *Kvantovaya Elektron*., **31** (1), 85 (2001) [*Quantum Electronics*, **31** (1), 85 (2001)].
9. Loussert C., Brasselet E. *Opt. Lett*., **35**, 7 (2010).
10. Khilo N.A. *Opt. Commun*., **285**, 503 (2012).
11. Khonina S.N., Morozov A.A., Karpeev S.V. *Laser Phys*., **24**, 056101 (2014).
12. Khonina S.N., Kharitonov S.I. *J. Modern Opt*., **62** (2), 125 (2015).
13. Koronkevich P., Mikhaltsova I.A., Churin E.G., Yurlov Yu.I. *Appl. Opt*., **34**, 5761 (1993).
14. Khonina S.N., Volotovsky S.G. *Computer Optics*, **33** (4), 401 (2009).